Reduced-Order Finite Element Models of Viscoelastically Damped Beams Through Internal Variables Projection

Marcelo A. Trindade
Department of Mechanical Engineering,
São Carlos School of Engineering,
University of São Paulo,
Av. Trabalhador São-Carlense, 400,
São Carlos-SP, 13566-590, Brazil
e-mail: trindade@sc.usp.br

For a growing number of applications, the well-known passive viscoelastic constrained layer damping treatments need to be augmented by some active control technique. However, active controllers generally require time-domain modeling and are very sensitive to system changes while viscoelastic materials properties are highly frequency dependent. Hence, effective methods for time-domain modeling of viscoelastic damping are needed. This can be achieved through internal variables methods, such as the anelastic displacements fields and the Golla-Hughes-McTavish. Unfortunately, they increase considerably the order of the model as they add dissipative degrees of freedom to the system. Therefore, the dimension of the resulting augmented model must be reduced. Several researchers have presented successful methods to reduce the state space coupled system, resulting from a finite element structural model combined with an internal variables viscoelastic model. The present work presents an alternative two-step reduction method for such problems. The first reduction is applied to the second-order model, through a projection of the dissipative modes onto the structural modes. It is then followed by a second reduction applied to the resulting coupled state space model. The reduced-order models are compared in terms of performance and computational efficiency for a cantilever beam with a passive constrained layer damping treatment. Results show a reduction of up to 67% of added dissipative degrees of freedom at the first reduction step leading to much faster computations at the second reduction step. [DOI: 10.1115/1.2202155]

1 Introduction

It is well known that viscoelastic constrained layer damping treatments can reduce resonant structural vibrations. For a growing number of applications, however, and due to material and/or geometrical limitations, this passive damping needs to be augmented by some active control technique. Indeed, several hybrid active-passive damping mechanisms were proposed in the last decade through the combination of piezoelectric-actuated active vibration control and viscoelastic damping treatments [1,2]. The main difficulty when associating active control and viscoelastic treatments is that active controllers are generally very sensitive to system changes while viscoelastic materials properties are highly frequency dependent. In addition, most modern control techniques require a time-domain model representation. Hence, effective methods for time-domain modeling of viscoelastic damping are needed. This can be achieved through internal variables methods, such as the anelastic displacements fields (ADF), proposed by Lesieutre and Bianchini [3], and the Golla-Hughes-McTavish (GHM), proposed by Golla and Hughes [4] and McTavish and Hughes [5], that allow effective time-domain modeling of the frequency dependence of stiffness and damping properties of viscoelastically damped structures. It was shown in [6] that both ADF and GHM are effective for time-domain analyses of highly damped structures. Unfortunately, they increase considerably the dimension of the resulting augmented model as they add dissipative degrees of freedom to the system. Therefore, the resulting model must be reduced.

There are mainly three strategies published in the literature for the reduction of viscoelastic finite element (FE) models with internal variables. The first one consists in applying some reduction method to the undamped structural FE model before adding the internal variables, which has the advantage of handling smaller matrices but generally leads to erroneous or less precise estimations of viscoelastic damping. This was shown by Friswell and Inman [7] who considered reducing the order of the physical FE model, through a system equivalent reduction expansion process, before and after assembly, previous to introducing the extra dissipative coordinates for the GHM method. The second reduction strategy consists in applying a reduction method to the second-order augmented FE model, after inclusion of internal variables. Park, Inman and Lam [8] have studied Guyan reduction method to reduce the order of a FE model augmented by GHM viscoelastic dissipative coordinates, but they showed that the method performs poorly. The third strategy is based on the application of a reduction method to the augmented state space system, that is after inclusion of the internal variables and transformation to the state space form. This has the advantage of allowing the application of modern reduction methods, developed for state space systems, such as internal balancing method. Friswell and Inman [7] and Park, Inman and Lam [8] applied an internal balancing method to a state space system augmented by GHM dissipative coordinates. Friswell and Inman [7] also applied eigensystem truncation for comparison. Trindade, Benjeddou and Ohayon [9] have also applied eigensystem truncation, followed by a real representation of the complex reduced system, to a state space system augmented by ADF dissipative coordinates. Both balanced realization and eigensystem truncation methods were shown to be effective in reducing the order of the state space system while retaining the viscoelastic damping behavior. However, they require a high computational effort due to a generally large dimension of augmented state space matrices.

The present work presents an alternative two-step reduction method for internal variables-based viscoelastic FE models. The

Contributed by the Technical Committee on Vibration and Sound of ASME for publication in the JOURNAL OF VIBRATION AND ACOUSTICS. Manuscript received September 15, 2004; final manuscript received January 24, 2006. Assoc. Editor: William W. Clark.

first reduction is applied to the second-order model, through a projection of the dissipative modes onto the structural modes. This approach also provides an effective measure of the coupling between the dissipative modes and structural modes, and enables physical interpretation of the former. The second-order model reduction is then followed by another reduction applied to the resulting coupled state space model. The objective is to allow a reduction of the extra dissipative coordinates before transformation to the state space, so as to provide faster computations on the reduction of the state space system.

2 Finite Element Model

Let us consider the following equations of motion for a finite element structural model

$$\mathbf{M}\ddot{\mathbf{q}} + \mathbf{D}\dot{\mathbf{q}} + [\mathbf{K}_e + \mathbf{K}_v]\mathbf{q} = \mathbf{F} \tag{1}$$

where $\mathbf{q}$ is the degrees of freedom (dof) vector and, $\dot{\mathbf{q}}$ and $\ddot{\mathbf{q}}$ are, respectively, the velocity and acceleration vectors. $\mathbf{M}$ is the mass matrix, $\mathbf{D}$ is a viscous damping matrix introduced a posteriori, and $\mathbf{F}$ is a mechanical perturbation input. $\mathbf{K}_v$ is the part of the stiffness matrix corresponding to the contribution of the viscoelastic material and $\mathbf{K}_e$ is the stiffness matrix corresponding to the remaining stiffness contributions in the structure.

The frequency dependence of the viscoelastic material properties is modeled through the ADF model [3]. The ADF model is based on a separation of the viscoelastic material strains in an elastic part, instantaneously proportional to the stress, and an anelastic (or dissipative) part, representing material relaxation. This could be applied to Eq. (1) by replacing the dof vector $\mathbf{q}$ by $\mathbf{q}^e = \mathbf{q} - \Sigma_i \mathbf{q}_i^d$ in the viscoelastic strain energy; where $\mathbf{q}^e$ and $\mathbf{q}_i^d$ represent the dof vectors associated with the elastic and anelastic strains, respectively. Adding a system of equations describing the time-domain evolution of the dissipative dof $\mathbf{q}_i^d$ to Eq. (1), we get

$$\mathbf{M}\ddot{\mathbf{q}} + \mathbf{D}\dot{\mathbf{q}} + (\mathbf{K}_e + \mathbf{K}_v^\infty)\mathbf{q} - \mathbf{K}_v^\infty \sum_i \mathbf{q}_i^d = \mathbf{F} \tag{2}$$

$$\frac{C_i}{\Omega_i}\mathbf{K}_v^\infty \dot{\mathbf{q}}_i^d + C_i \mathbf{K}_v^\infty \mathbf{q}_i^d - \mathbf{K}_v^\infty \mathbf{q} = \mathbf{0} \tag{3}$$

where $\mathbf{K}_v^\infty = G_\infty \bar{\mathbf{K}}_v$, for $G_\infty = G_0(1+\Sigma_i \Delta_i)$ and $C_i = (1+\Sigma_i \Delta_i)/\Delta_i$ [3]. ADF parameters G_0, Δ_i and Ω_i are evaluated by curve fitting of the measurements of $G^*(\omega)$, represented as a series of functions in the frequency domain

$$G^*(\omega) = G_0 + G_0 \sum_i \Delta_i \frac{\omega^2 + \mathrm{j}\omega\Omega_i}{\omega^2 + \Omega_i^2} \tag{4}$$

The form of the series of functions used to construct $G^*(\omega)$ is well adapted to fit the behavior of complex modulus frequency dependence for generic viscoelastic materials, which present strong frequency dependence. Nevertheless, modern viscoelastic materials tend to be less frequency dependent so as to maintain a high loss factor over a wide frequency range of interest, and consequently being more effective in damping vibrations. For such materials, a larger number of series terms must be used to provide a satisfactory curve fit of complex modulus frequency dependence. A more detailed analysis of curve fitting will be presented later, but it is worthwhile advancing that, for modern viscoelastic materials used for vibration damping, more than three ADF series terms are generally required and the larger the number of ADF series terms considered the better fitting of materials properties is obtained. Notice, however, that there is one system of equations (Eq. (3)) for each ADF series term considered. Thus, there must be a compromise between the quality of material properties curve fitting and the number of extra systems of equations included into the final augmented system. Since the extra dissipative dof $\mathbf{q}_i^d$ included for each ADF series term has the same dimension of $\mathbf{q}$, the dimension of the final augmented system will be at least four times that of the original FE system (considering three ADF series terms to represent frequency dependence behavior).

It is worthwhile to notice also that in the case of a structure partially covered with the viscoelastic treatment, the viscoelastic stiffness matrix $\mathbf{K}_v^\infty$ will possess a number of rigid body modes, corresponding to the FE dof of the nontreated parts of the structure. Consequently, there will be a number of equations in Eq. (3) that will be automatically satisfied. Hence, the increase in the augmented system dimension will be also dependent on the percent of area covered with the viscoelastic material throughout the structure surface.

The rigid body modes of $\mathbf{K}_v^\infty$ can be eliminated through a modal decomposition $\mathbf{q}_i^d = \mathbf{T}_d \hat{\mathbf{q}}_i^d$, such that $\Lambda_d = \mathbf{T}_d^T \mathbf{K}_v^\infty \mathbf{T}_d$ and Eqs. (2) and (3) can be rewritten as

$$\mathbf{M}\ddot{\mathbf{q}} + \mathbf{D}\dot{\mathbf{q}} + (\mathbf{K}_e + \mathbf{K}_v^\infty)\mathbf{q} - \mathbf{T}_d \Lambda_d \sum_i \hat{\mathbf{q}}_i^d = \mathbf{F} \tag{5}$$

$$\frac{C_i}{\Omega_i}\Lambda_d \dot{\hat{\mathbf{q}}}_i^d + C_i \Lambda_d \hat{\mathbf{q}}_i^d - \Lambda_d \mathbf{T}_d^T \mathbf{q} = \mathbf{0} \tag{6}$$

The equations that are automatically satisfied correspond to the null eigenvalues in matrix Λ_d. Notice that these rigid body modes of $\mathbf{K}_v^\infty$ do not contribute to the overall structural damping. Hence, the null eigenvalues are eliminated from Λ_d and so are the corresponding eigenvectors from $\mathbf{T}_d$. The combination of Eqs. (5) and (6) leads to the following augmented system

$$\bar{\mathbf{M}}\ddot{\bar{\mathbf{q}}} + \bar{\mathbf{D}}\dot{\bar{\mathbf{q}}} + \bar{\mathbf{K}}\bar{\mathbf{q}} = \bar{\mathbf{F}} \tag{7}$$

with

$$\bar{\mathbf{M}} = \begin{bmatrix} \mathbf{M} & \mathbf{0} \\ \mathbf{0} & \mathbf{0} \end{bmatrix}; \quad \bar{\mathbf{D}} = \begin{bmatrix} \mathbf{D} & \mathbf{0} \\ \mathbf{0} & \mathbf{D}_{dd} \end{bmatrix}; \quad \bar{\mathbf{F}} = \begin{Bmatrix} \mathbf{F} \\ \mathbf{0} \end{Bmatrix}$$

$$\bar{\mathbf{K}} = \begin{bmatrix} \mathbf{K}_e + \mathbf{K}_v^\infty & \mathbf{K}_{ed} \\ \mathbf{K}_{ed}^T & \mathbf{K}_{dd} \end{bmatrix}; \quad \bar{\mathbf{q}} = \mathrm{col}(\mathbf{q}, \hat{\mathbf{q}}_1^d, \ldots, \hat{\mathbf{q}}_n^d)$$

where

$$\mathbf{D}_{dd} = \mathrm{diag}\left(\frac{C_1}{\Omega_1}\Lambda_d \cdots \frac{C_n}{\Omega_n}\Lambda_d\right); \quad \mathbf{K}_{dd} = \mathrm{diag}(C_1\Lambda_d \cdots C_n\Lambda_d);$$

$$\mathbf{K}_{ed} = [-\mathbf{T}_d\Lambda_d \cdots -\mathbf{T}_d\Lambda_d]$$

3 State Space Model Construction

In order to eliminate the apparent singularity of the mass matrix of system (7) and to provide a transformation to an "elastic only" modal reduced model, Eq. (7) is rewritten in a state space form. Therefore, a state vector $\mathbf{x}$ is formed by the augmented vector $\bar{\mathbf{q}}$ and the time derivative of the mechanical dof vector $\dot{\mathbf{q}}$. The time derivatives of the dissipative dof $\mathbf{q}_i^d$ are not included in the state vector since these variables are massless. This leads to

$$\dot{\mathbf{x}} = \mathbf{A}\mathbf{x} + \mathbf{p}; \; \mathbf{y} = \mathbf{C}\mathbf{x} \tag{8}$$

where the perturbation vector $\mathbf{p}$ is the state distribution of the mechanical loads $\mathbf{F}$ and the output vector $\mathbf{y}$ is, generally, composed of the measured quantities, written in terms of the state vector $\mathbf{x}$ through the output matrix $\mathbf{C}$. The system dynamics is determined by the square matrix $\mathbf{A}$. These are

$$\mathbf{A} = \begin{bmatrix} \mathbf{0} & \mathbf{0} & \cdots & \mathbf{0} & \mathbf{I} \\ \frac{\Omega_1}{C_1}\mathbf{T}_d^T & -\Omega_1\mathbf{I} & & \mathbf{0} & \mathbf{0} \\ \vdots & & \ddots & & \mathbf{0} \\ \frac{\Omega_n}{C_n}\mathbf{T}_d^T & \mathbf{0} & & -\Omega_n\mathbf{I} & \mathbf{0} \\ -\mathbf{M}^{-1}(\mathbf{K}_e + \mathbf{K}_v^\infty) & \mathbf{M}^{-1}\mathbf{T}_d\Lambda_d & \cdots & \mathbf{M}^{-1}\mathbf{T}_d\Lambda_d & -\mathbf{M}^{-1}\mathbf{D} \end{bmatrix}$$

$$\mathbf{x}=\begin{bmatrix}\bar{\mathbf{q}}\\ \dot{\mathbf{q}}\end{bmatrix};\quad \mathbf{p}=\begin{bmatrix}\mathbf{0}\\ \mathbf{M}^{-1}\mathbf{F}\end{bmatrix};\quad \mathbf{C}=[\mathbf{C}_{\bar{q}}\ \mathbf{C}_{\dot{q}}]$$

where $\mathbf{C}_{\bar{q}}$ and $\mathbf{C}_{\dot{q}}$ are output matrices relative to augmented dof vector $\bar{\mathbf{q}}$ and mechanical dof derivatives $\dot{\mathbf{q}}$, respectively.

4 Model Reduction

It is evident from Eq. (7) that inclusion of dissipative dof greatly increases the dimension of the FE model, even for a partial treatment, corresponding to a great increase also in the final state space model (Eq. (8)). Since our final objective is to apply the state space model for control design and optimization, leading to CPU-demanding computations for a large number of candidate configurations, some model reduction is required. Hence, in this section some techniques are presented to provide an reduced-order state space model, which dimension is small enough to allow application to control design and optimization and that is still able to well represent the viscoelastic damping of the structure.

4.1 State Space Model Reduction. In principle, all reduction techniques for state space systems may be applied to Eq. (8). The most standard ones are the reduction to modal coordinates and the reduction via internal balancing methods. While the latter leads to more precise results for a given input and output configuration, the former is independent of input and output configurations and also allow faster computations. Details on reduction via internal balancing methods can be found in [8]. Details on modal reduction can be found in [9] and are briefly resumed in this section.

By neglecting the contributions of viscoelastic relaxation modes and some elastic modes, related to eigenfrequencies out of the frequency-range considered, a complex-based modal reduction can be applied to the state space system (8). The eigenvalues matrix Λ and, left $\mathbf{T}_l$ and right $\mathbf{T}_r$, eigenvectors of Eq. (8) are first evaluated from

$$\mathbf{A}\mathbf{T}_r=\Lambda\mathbf{T}_r;\quad \mathbf{A}^T\mathbf{T}_l=\Lambda\mathbf{T}_l \tag{9}$$

so that $\mathbf{T}_l^T\mathbf{T}_r=\mathbf{I}$, then decomposed as following

$$\Lambda=\begin{bmatrix}\Lambda_r & \mathbf{0} & \mathbf{0}\\ \mathbf{0} & \Lambda_{ne} & \mathbf{0}\\ \mathbf{0} & \mathbf{0} & \Lambda_{nd}\end{bmatrix};\quad \mathbf{T}_l=[\mathbf{T}_{lr}\ \mathbf{T}_{lne}\ \mathbf{T}_{lnd}];$$
$$\mathbf{T}_r=[\mathbf{T}_{rr}\ \mathbf{T}_{rne}\ \mathbf{T}_{rnd}] \tag{10}$$

The state vector is then approximated as $\mathbf{x}\approx\mathbf{T}_{rr}\mathbf{x}_r$, so that the contribution of out-of-frequency-range elastic and viscoelastic relaxation modes $\mathbf{T}_{lne}$, $\mathbf{T}_{rne}$, $\mathbf{T}_{lnd}$ and $\mathbf{T}_{rnd}$ is neglected. Hence, the system (8) may be reduced to

$$\dot{\mathbf{x}}_r=\Lambda_r\mathbf{x}_r+\mathbf{T}_{lr}^T\mathbf{p}\quad \mathbf{y}=\mathbf{C}\mathbf{T}_{rr}\mathbf{x}_r \tag{11}$$

The main disadvantage of the reduced state space system (11) is that its matrices are complex. Fortunately, since all overdamped (relaxation) modes were neglected, all elements of the system (11) are composed of complex conjugates, such that it is possible to use a state transformation $\hat{\mathbf{x}}=\mathbf{T}_c\mathbf{x}_r$ [10] and write the following real state space system equivalent to Eq. (11)

$$\dot{\hat{\mathbf{x}}}=\hat{\mathbf{A}}\hat{\mathbf{x}}+\hat{\mathbf{p}}\quad \mathbf{y}=\hat{\mathbf{C}}\hat{\mathbf{x}} \tag{12}$$

where

$$\hat{\mathbf{A}}=\mathbf{T}_c\Lambda_r\mathbf{T}_c^{-1}=\begin{bmatrix}\mathbf{0} & & & \mathbf{I}\\ \ddots & & \ddots & \\ & -|\lambda_j|^2 & 2\Re(\lambda_j) & \\ & \ddots & & \ddots\end{bmatrix}$$
$$\hat{\mathbf{p}}=\mathbf{T}_c\mathbf{T}_{lr}^T\mathbf{p};\quad \hat{\mathbf{C}}=\mathbf{C}\mathbf{T}_{rr}\mathbf{T}_c^{-1}$$

It is clear that the eigenvalues of the real matrix $\hat{\mathbf{A}}$ are exactly the elements of Λ_r, i.e. the retained elastic eigenvalues λ_j and their complex conjugates $\bar{\lambda}_j$. In the form of Eq. (12), the new state variables $\hat{\mathbf{x}}$ represent the modal displacements and velocities.

4.2 Second-Order Model Reduction. The main difficulty in using reduction methods for state space systems, either via modal truncation or balanced realization, is that the dimension of the state space matrix $\mathbf{A}$ may be very large due to the inclusion of internal variables in the FE model. Consequently, when there is a need for repeating the reduced model evaluation for several treatment configurations, which is often the case for control design and optimization, it easily becomes an impractical task. Hence, a novel model reduction method is presented in this section. It consists in reducing the dissipative system (Eq. (6)) before construction of the augmented state space system. Since Eq. (6) is already constructed in terms of a modal decomposition of the viscoelastic stiffness matrix $\mathbf{K}_v^\infty$, that is, in terms of viscoelastic dissipative modes, one could consider retaining only a few dissipative modes to reduce the augmented system dimension. Obviously, the difficulty would be to guess which dissipative modes to retain.

Let us suppose that the damped solution for the FE dof may be written as $\mathbf{q}=\mathbf{T}_e\hat{\mathbf{q}}$. Replacing this expression in Eq. (6) leads to

$$\mathbf{T}_e^T\mathbf{M}\mathbf{T}_e\ddot{\hat{\mathbf{q}}}+\mathbf{T}_e^T\mathbf{D}\mathbf{T}_e\dot{\hat{\mathbf{q}}}+\mathbf{T}_e^T(\mathbf{K}_e+\mathbf{K}_v^\infty)\mathbf{T}_e\hat{\mathbf{q}}-\mathbf{T}_e^T\mathbf{T}_d\Lambda_d\sum_i\hat{\mathbf{q}}_i^d=\mathbf{T}_e^T\mathbf{F} \tag{13}$$

$$\frac{C_i}{\Omega_i}\Lambda_d\dot{\hat{\mathbf{q}}}_i^d+C_i\Lambda_d\hat{\mathbf{q}}_i^d-\Lambda_d\mathbf{T}_d^T\mathbf{T}_e\hat{\mathbf{q}}=\mathbf{0} \tag{14}$$

Since the null eigenvalues were eliminated from Λ_d, Eq. (14) could also be written as

$$\dot{\hat{\mathbf{q}}}_i^d=-\Omega_i\hat{\mathbf{q}}_i^d+\frac{\Omega_i}{C_i}\mathbf{T}_d^T\mathbf{T}_e\hat{\mathbf{q}} \tag{15}$$

Notice from the last equation that the jkth element of the matrix $\mathbf{T}_d^T\mathbf{T}_e$ represents the contribution of the kth response mode to the jth dissipative mode of the viscoelastic substructure, that is, a measure of how the kth response mode excites the jth mode of the viscoelastic substructure. Consequently, supposing that the energy of the overall response is concentrated in certain "response modes," we might be able to identify the dissipative modes which are the most excited by the response. Alternatively, from Eq. (13), one may notice that the elements of matrix $\mathbf{T}_e^T\mathbf{T}_d\Lambda_d$ also give a measure of how each viscoelastic dissipative mode contributes to the structural response. Hence, a technique was tested to select some viscoelastic dissipative modes based on their contribution to the dynamics of the overall structure.

Let us define the matrix $\mathbf{R}$ as

$$\mathbf{R}=\Lambda_d\mathbf{T}_d^T\mathbf{T}_e \tag{16}$$

such that its elements R_{jk} represent the weighted residuals between viscoelastic dissipative mode $\mathbf{T}_d^j$ and response mode $\mathbf{T}_e^k$. Supposing that the majority of structural response energy is contained in the $\{N_k\}$ modes in $\mathbf{T}_e$, the selection of the dissipative modes that contribute the most to the structural response may be performed through the sorting of the following residual vector $\mathbf{r}$

$$r_j=\|R_{jk}\|,\quad \text{for } k\in\{N_k\} \tag{17}$$

Notice that each element of $\mathbf{r}$ corresponds to a column of $\mathbf{T}_d$, that is a viscoelastic dissipative mode. Thus, it is proposed to eliminate the dissipative modes from $\mathbf{T}_d$ corresponding to the smallest residuals r_j, which are thought to be those that contribute the least to the structural response. This is done through the following decomposition

$$\Lambda_d = \begin{bmatrix} \Lambda_{dr} & \mathbf{0} \\ \mathbf{0} & \Lambda_{dn} \end{bmatrix}; \quad \mathbf{T}_d = [\mathbf{T}_{dr}\ \mathbf{T}_{dn}] \tag{18}$$

where Λ_{dr} contains the eigenvalues of the $\{N_j\}$ dissipative modes with the largest residuals r_j. $\mathbf{T}_{dr}$ contains the corresponding eigenvectors, that are the dissipative modes to be retained in the model. The other dissipative modes $\mathbf{T}_{dn}$ and their corresponding eigenvalues Λ_{dn} are then neglected. Therefore, the dissipative dof is approximated by $\mathbf{q}_i^d \approx \mathbf{T}_{dr}\hat{\mathbf{q}}_i^{dr}$. The reduced modal matrix $\mathbf{T}_{dr}$ contains thus only the retained dissipative modes and $\hat{\mathbf{q}}_i^{dr}$ are their corresponding coordinates. Since the eigenvalues matrix is also reduced to Λ_{dr}, the residual matrix becomes $\mathbf{R}_r = \Lambda_{dr}\mathbf{T}_{dr}^T\mathbf{T}_e$.

Two main factors determine the performance of the proposed reduction technique: (1) the basis considered for the structural response $\mathbf{T}_e$ and (2) the number of dissipative modes kept in the model. As for the basis considered, let us suppose as a first approximation that the damped modes are similar to the undamped modes. Then, assuming that $\mathbf{T}_e^T\mathbf{M}\mathbf{T}_e = \mathbf{I}$ and $\mathbf{T}_e^T(\mathbf{K}_e + \mathbf{K}_v^\infty)\mathbf{T}_e = \Lambda_e$, Eqs. (13) and (14) can be rewritten as

$$\ddot{\hat{\mathbf{q}}} + \mathbf{T}_e^T\mathbf{D}\mathbf{T}_e\dot{\hat{\mathbf{q}}} + \Lambda_e\hat{\mathbf{q}} - \mathbf{R}_r^T\sum_i \hat{\mathbf{q}}_i^{dr} = \mathbf{T}_e^T\mathbf{F} \tag{19}$$

$$\frac{C_i}{\Omega_i}\Lambda_{dr}\dot{\hat{\mathbf{q}}}_i^{dr} + C_i\Lambda_{dr}\hat{\mathbf{q}}_i^{dr} - \mathbf{R}_r\hat{\mathbf{q}} = \mathbf{0} \tag{20}$$

The combination of Eqs. (19) and (20) leads then to a reduced-order augmented system

$$\bar{\mathbf{M}}\ddot{\bar{\mathbf{q}}} + \bar{\mathbf{D}}\dot{\bar{\mathbf{q}}} + \bar{\mathbf{K}}\bar{\mathbf{q}} = \bar{\mathbf{F}} \tag{21}$$

with

$$\bar{\mathbf{M}} = \begin{bmatrix} \mathbf{I} & \mathbf{0} \\ \mathbf{0} & \mathbf{0} \end{bmatrix}; \quad \bar{\mathbf{D}} = \begin{bmatrix} \mathbf{T}_e^T\mathbf{D}\mathbf{T}_e & \mathbf{0} \\ \mathbf{0} & \mathbf{D}_{dd} \end{bmatrix}; \quad \bar{\mathbf{F}} = \begin{bmatrix} \mathbf{T}_e^T\mathbf{F} \\ \mathbf{0} \end{bmatrix}$$

$$\bar{\mathbf{K}} = \begin{bmatrix} \Lambda_e & \mathbf{K}_{ed} \\ \mathbf{K}_{ed}^T & \mathbf{K}_{dd} \end{bmatrix}; \quad \bar{\mathbf{q}} = \mathrm{col}(\hat{\mathbf{q}}, \hat{\mathbf{q}}_1^{dr}, \ldots, \hat{\mathbf{q}}_n^{dr})$$

where

$$\mathbf{D}_{dd} = \mathrm{diag}\left(\frac{C_1}{\Omega_1}\Lambda_{dr} \cdots \frac{C_n}{\Omega_n}\Lambda_{dr}\right);$$

$$\mathbf{K}_{dd} = \mathrm{diag}(C_1\Lambda_{dr} \cdots C_n\Lambda_{dr}); \quad \mathbf{K}_{ed} = [-\mathbf{R}_r^T \cdots -\mathbf{R}_r^T]$$

Notice that the structural model could be, but is not, reduced using its undamped modes $\mathbf{T}_e$, although writing the equations in terms of $\hat{\mathbf{q}}$ instead of $\mathbf{q}$ has some advantages, such as to provide a diagonal structural model, specially if damping matrix $\mathbf{D}$ is a proportional damping such $\bar{\mathbf{D}}$ will be a diagonal matrix. However, the same technique for reducing the dimension of the dissipative system could still be used with a nondiagonal structural model in Eq. (21). Notice also, from Eq. (21), that the reduced dissipative coordinates $\hat{\mathbf{q}}_i^{dr}$ contain now only those coordinates corresponding to the selected dissipative modes according to their residual and, thus, matrices $\mathbf{R}_r$ and Λ_{dr} have a reduced dimension. This reduction can be specially important since each eliminated dissipative mode leads to a reduction of n dof in Eq. (21), where n is the number of ADF series terms considered (generally at least three).

The state space system matrices and vectors of Eq. (8) can then be rewritten as

$$\mathbf{A} = \begin{bmatrix} \mathbf{0} & \mathbf{0} & \cdots & \mathbf{0} & \mathbf{I} \\ \frac{\Omega_1}{C_1}\mathbf{T}_{dr}^T\mathbf{T}_e & -\Omega_1\mathbf{I} & & \mathbf{0} & \mathbf{0} \\ \vdots & & \ddots & & \mathbf{0} \\ \frac{\Omega_n}{C_n}\mathbf{T}_{dr}^T\mathbf{T}_e & \mathbf{0} & & -\Omega_n\mathbf{I} & \mathbf{0} \\ -\Lambda_e & \mathbf{R}_r^T & \cdots & \mathbf{R}_r^T & -\mathbf{T}_e^T\mathbf{D}\mathbf{T}_e \end{bmatrix}$$

$$\mathbf{x} = \begin{bmatrix} \bar{\mathbf{q}} \\ \dot{\bar{\mathbf{q}}} \end{bmatrix}; \quad \mathbf{p} = \begin{bmatrix} \mathbf{0} \\ \mathbf{T}_e^T\mathbf{F} \end{bmatrix}; \quad \mathbf{C} = [\mathbf{C}_{\bar{q}}\mathbf{T}_e\ \mathbf{C}_{\dot{q}}\mathbf{T}_e]$$

These, now reduced, state space system matrices can then be further reduced through the state space model reduction presented previously, saving a large amount of computation effort. In the next section, the technique presented here is validated for a cantilever beam with viscoelastic treatment. Also an analysis of the number of dissipative modes that should be kept in the model is presented.

5 Validation of Reduced-Order Models

Let us consider the aluminum cantilever beam partially covered with a constrained layer treatment as presented in Fig. 1. The beam is of length 300 mm and thickness 1 mm and is made of aluminum with Young's modulus 70 GPa and mass density 2700 kg/m^3. No viscous damping is considered in this example, that is $\mathbf{D}=\mathbf{0}$. The constraining layer is also made of aluminum and has thickness 0.5 mm and length 270 mm, that is the treatment covers 90% of the beam and is centered. The viscoelastic layer has thickness 0.254 mm (10 mil) and is made of 3M ISD112 viscoelastic material, with a mass density of 1000 kg/m^3. The viscoelastic material shear modulus is frequency dependent. The curve fitting of ADF parameters to the measured shear modulus provided by 3M is presented in the next section.

5.1 Curve Fitting of Viscoelastic Material Properties. The ADF parameters G_∞, C_i and Ω_i needed to build system (8) are based on ADF relaxation function parameters G_0, Δ_i and Ω_i, from Eq. (4), which must be curve fitted relative to the measurements of $G^*(\omega)$. In the present work, a nonlinear least squares optimization method was used to evaluate the ADF parameters. Figure 2 shows the measured and approximated storage modulus (G') and loss factor (η) for 3M ISD112 viscoelastic material at 20°C, where

$$G^*(\omega) = G'(\omega) + \mathrm{j}G''(\omega) = G'(\omega)[1 + \mathrm{j}\,\eta(\omega)] \tag{22}$$

As shown in Fig. 2, both storage modulus and loss factor are well represented by five series terms of ADF parameters, whereas three ADF series terms provide only a first approximation (within 15% error margin) for the frequency dependence. Nevertheless, these parameters are valid only in the frequency range considered, that is, the frequency range for which material properties were furnished by 3M. Therefore, it is necessary to ensure a reasonable behavior of estimated material properties outside the frequency range, since arbitrary external perturbations will generally excite modes lying on this interval. Required asymptotical properties are

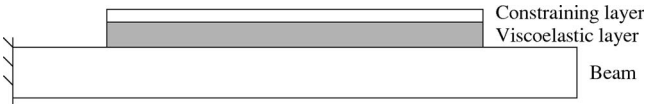

Fig. 1 Cantilever beam partially covered with a passive constrained layer damping treatment

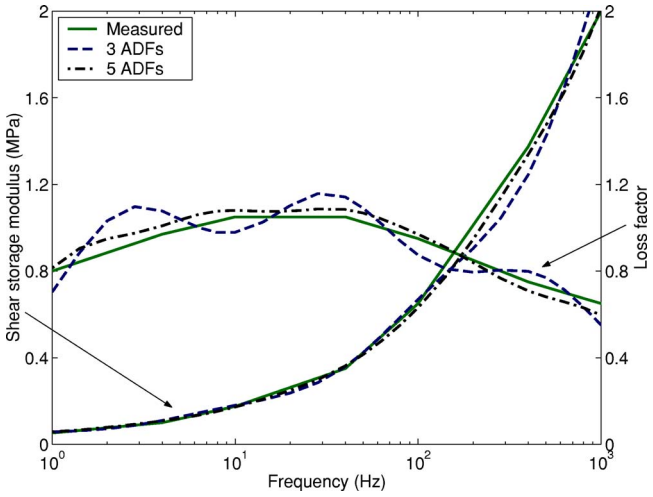

Fig. 2 Frequency dependence of 3M ISD112 viscoelastic material properties at 20°C (solid line) and curve fit using three (dashed line) and five (dashed-dotted line) ADF series terms

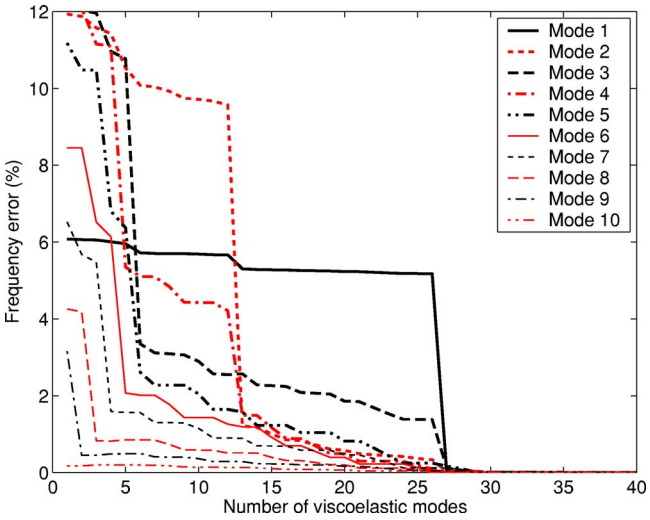

Fig. 3 Eigenfrequency error when using different numbers of dissipative modes in second-order system compared to using all but rigid body modes

$$\begin{cases} \lim_{\omega\to 0} G^*(\omega) = G_0 \\ \lim_{\omega\to\infty} G^*(\omega) = G_\infty \end{cases}, \quad \text{where } G_\infty > G_0 \in \mathbb{R}^+ \tag{23}$$

Meaning that the shear modulus tends to its static (relaxed) and instantaneous (unrelaxed) values at the boundaries 0 and ∞, respectively. This also imposes that $\eta(0), \eta(\infty)=0$, that is, dissipation only occurs in the transition region. Curve-fitted ADF parameters for viscoelastic material 3M ISD112 at 20°C respecting asymptotical behavior are presented in Table 1.

Notice also that these properties are valid for a temperature of 20°C and it is well known that temperature decrease will move these master curves to the left and vice versa. On the other hand, some viscoelastic materials present optimal loss factor at lower frequencies. So that it is normally possible to select a material according to frequency range of interest and operation temperature.

5.2 Comparison of Reduced- and Full-Order Viscoelastic Models. The reduced state space systems, with and without previous reduction of the dissipative system, are now compared for the cantilever beam introduced previously. This is done using a FE model considering 35 sandwich beam elements, with 6 dof per element, thus leading to a total of 105 mechanical dof (for details on the FE model, please refer to [11]). Five ADF series terms were considered in both cases, leading to an inclusion of 445 dissipative dof (89 dof × 5 ADF series terms) in addition to the 105 mechanical dof from the FE model.

Figures 3 and 4 present the eigenfrequency and modal damping factor errors, respectively, when using different numbers of dissipative modes prior to state space modal reduction compared to using all but rigid body dissipative modes. These selected dissipative modes correspond to the ones with largest residuals. Comparison of Figs. 3 and 4 shows that eigenfrequency errors are much smaller than damping factors errors. This is probably due to the fact that the dissipative coordinates are solely responsible for the damping in the structure and neglecting all dissipative modes leads to the absence of damping. Moreover, although the damping factor error decreases quite rapidly for modes 5–10, it is still larger than 20% for modes 1 and 3 when using less than 20 dissipative modes. Nevertheless, when using 30 dissipative modes the damping factor errors decrease to $\{0.06, 0.08, 0.09, 0.11, 0.12, 0.14, 0.16, 0.19, 0.24, 0.31\}$%, respectively, while the maximum eigenfrequency error is as low as 0.01%.

From Figs. 3 and 4, one may notice that both eigenfrequency and damping factor errors decay is achieved through a series of large steps. This can be explained by the fact that the damping factor of a specific vibration mode will be well represented only when a set of dissipative modes with strong coupling with this specific vibration mode is included. Since dissipative modes are sorted in terms of their weighted residuals, the inclusion of a few first dissipative modes with weak coupling with one or more vibration modes will not affect their damping factors. For example,

Table 1 Curve-fitted ADF parameters for viscoelastic material 3M ISD112 at 20°C

	3 ADF series terms			5 ADF series terms		
i	G_0 (MPa)	Δ_i	Ω_i (rad/s)	G_0 (MPa)	Δ_i	Ω_i (rad/s)
1	0.0511	2.8164	31.1176	0.0440	1.3545	12.4547
2		13.1162	446.4542		3.2610	73.8749
3		45.4655	5502.5318		7.7741	387.4302
4		–	–		18.9495	1472.7588
5		–	–		49.7732	9791.3957

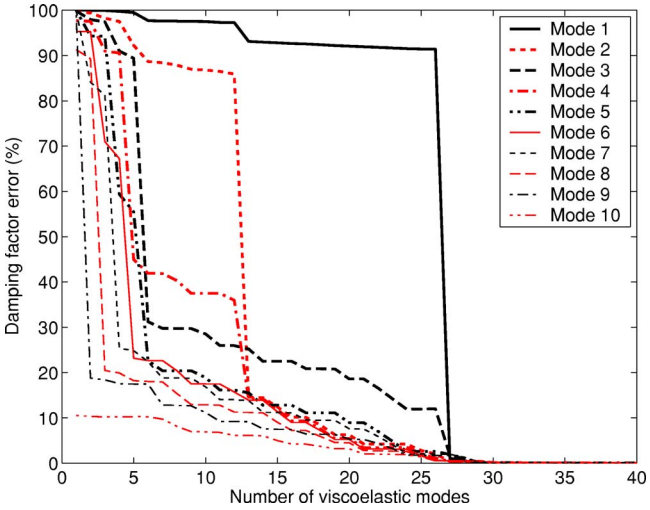

Fig. 4 Damping factor error when using different numbers of dissipative modes in second-order system compared to using all but rigid body modes

Table 2 Eigenfrequencies and damping factors for different levels of reduction

Full model, 89 dissipative modes		Reduction to 29 dissipative modes		Reduction to 19 dissipative modes		Reduction to 9 dissipative modes	
Eigenfrequencies and damping factors, Hz(%)							
16.1	(5.77)	16.1	(5.77)	16.9	(0.45)	17.0	(0.14)
90.6	(11.23)	90.6	(11.18)	91.2	(10.52)	99.5	(1.46)
235.1	(11.67)	235.1	(11.66)	239.9	(9.24)	242.3	(8.21)
422.5	(11.79)	422.7	(11.74)	424.6	(11.15)	441.3	(7.37)
649.3	(11.58)	649.3	(11.56)	656.0	(10.29)	664.0	(9.21)
916.5	(10.76)	916.8	(10.71)	920.1	(10.19)	929.6	(8.87)
1224.0	(9.37)	1224.1	(9.35)	1231.1	(8.48)	1239.8	(7.61)
1570.8	(7.79)	1571.1	(7.76)	1574.0	(7.43)	1580.0	(6.78)
1956.7	(6.32)	1956.9	(6.30)	1960.5	(5.92)	1964.5	(5.52)
2382.7	(5.08)	2382.9	(5.06)	2384.3	(4.92)	2386.1	(4.73)
Number of dissipative dof (added to second-order system)							
445		145		95		45	
Total number of dof (second-order system)							
550		250		200		150	

it seems for this example that the coupling between the 26 first sorted dissipative modes and the first vibration mode is not very strong (but it is for the other vibration modes). That is why the damping factor error for the first vibration mode is reduced from 91% to 1% when the 27th dissipative mode is included (Fig. 4). On the other hand, the damping factor error for the tenth vibration mode is decreased gradually by the inclusion of a set of dissipative modes.

Table 2 shows the eigenfrequencies and damping factors for different levels of reduction of dissipative modes. It is clear that the reduction to 29 dissipative modes (of the 89 available) leads to an accurate representation of the eigenfrequencies and damping factors. Indeed, from Fig. 5, one can observe that the 31st largest residual is only 0.6% of the first one so that most of the coupling between elastic and dissipative coordinates is provided by the first 30 dissipative modes. Alternatively, one may also observe, from Fig. 5, that the cumulative sum of the normalized residuals is more than 99% for 30 dissipative modes.

Figure 6 shows the frequency response function between the impact force input and displacement output, both colocated at 10 mm from the clamped end, using all but rigid body dissipative modes, as a reference, and reduced-order models using only 9, 19 and 29 dissipative modes of the 89 available. It is possible to observe that higher-frequency modes are better represented by low-order models as previously shown in frequency and damping errors analyses. It can be seen, however, that, when using only nine dissipative modes, the frequency response around the first, second, and fourth eigenfrequencies is not correctly represented. However, when including 19 dissipative modes, the difference between the reduced-order model and the full-dissipative model is almost only perceptible around the first eigenfrequency. The frequency response for the reduced-order model with 29 dissipative modes matches almost exactly the full-dissipative model.

As it is guessed that the importance of the dissipative coordinates in the representation of damping may be dependent on the overall damping level induced in the structure by the viscoelastic damping treatment, a similar analysis was performed for a cantilever beam with only 50% of area covered with the viscoelastic treatment. This is done by changing the length of the viscoelastic and constraining layers to 150 mm in Fig. 1, whereas still centered in the beam surface. This leads to a much less damped structure, such that the ten first modal damping factors are $\zeta(50\%)=[5.6,9.2,5.3,5.2,6.7,5.3,4.7,4.7,3.8,2.8]\%$ compared to $\zeta(90\%)=[5.8,11.2,11.7,11.8,11.6,10.8,9.4,7.8,6.3,5.1]\%$

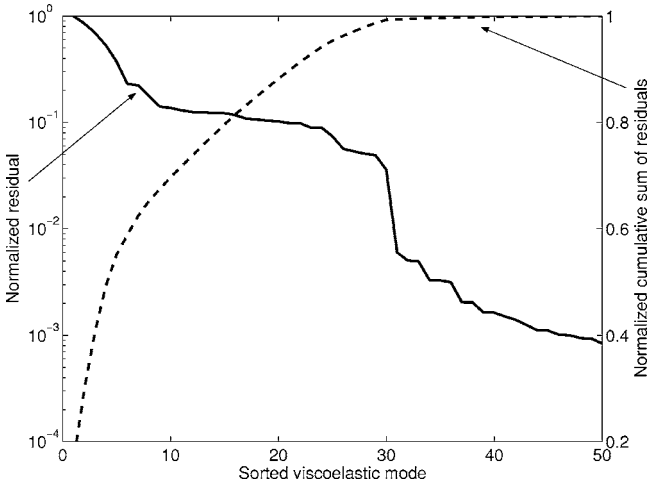

Fig. 5 Normalized residual and cumulative sum of residuals for the viscoelastic dissipative modes

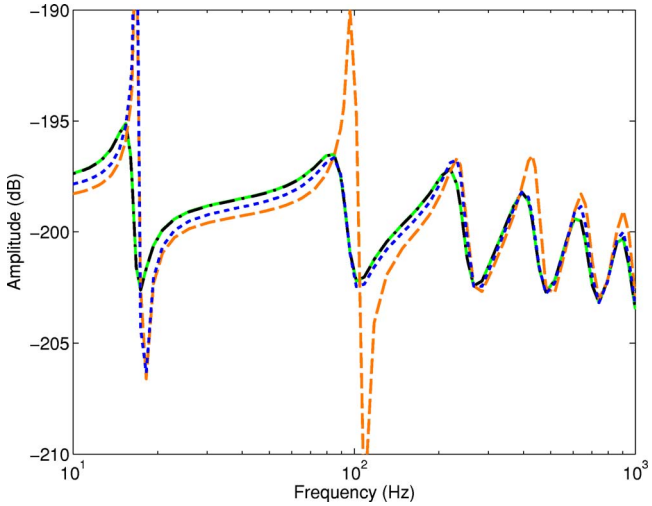

Fig. 6 Frequency response function using different numbers of dissipative modes in second-order system. –: all but rigid body modes (89), – –: 9 modes, - - -: 19 modes, –.–: 29 modes

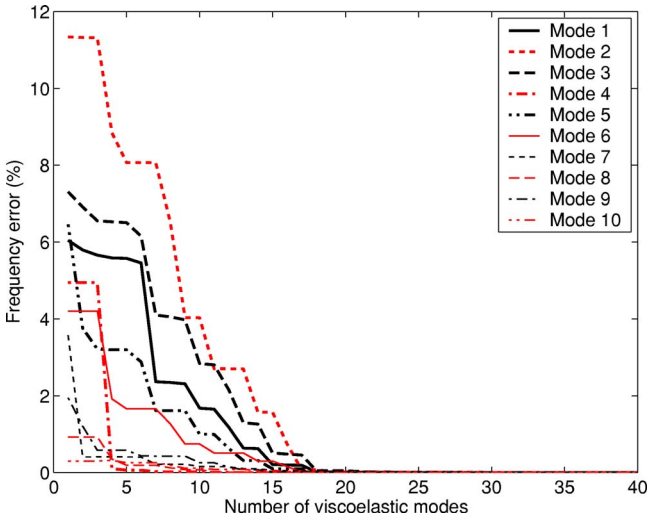

Fig. 7 Eigenfrequency error when using different numbers of dissipative modes in second-order system compared to using all but rigid body modes

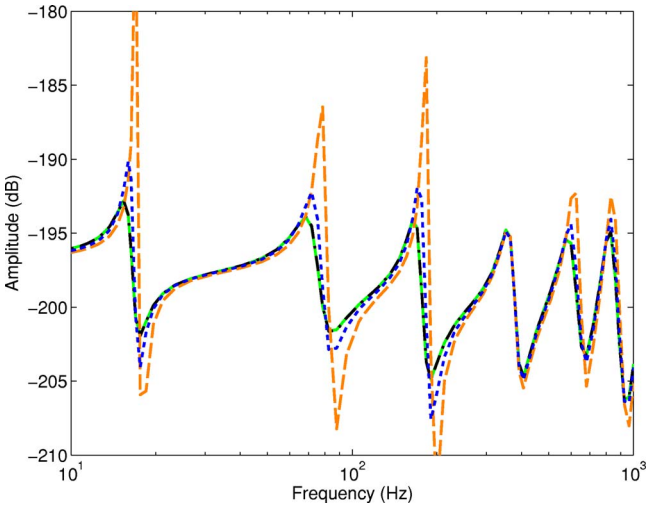

Fig. 9 Frequency response function using different numbers of dissipative modes in second-order system. –: all but rigid body modes (52), – –: 5 modes, - - -: 9 modes, –.–: 18 modes

of the previous configuration.

Similarly to the previous case, Figs. 7 and 8 present the eigenfrequency and modal damping factor errors, respectively, when using different numbers of dissipative modes compared to using all but rigid body dissipative modes. For this case, the eigenfrequency errors are also much smaller than that for the damping factors. Here, both the eigenfrequency and damping factor errors decrease more rapidly than in the previous case. It may be guessed that this is due to the fact that a less damped structure requires less dissipative coordinates. Indeed, in this case, only 18 dissipative modes are required to reduce the damping error to less than 1% for all ten first vibration modes. Indeed, when using 18 dissipative modes, the damping factor errors are $\{0.75, 0.87, 0.66, 0.01, 0.14, 0.28, 0.20, 0.10, 0.17, 0.36\}\%$, respectively, and the maximum eigenfrequency error is 0.07%. Also, as in the previous case, the cumulative sum of the normalized residuals is more than 99%.

For the case of 50% coverage, the frequency response function was also analyzed, and it is shown in Fig. 9, using all but rigid body dissipative modes, as a reference, and reduced-order models using only 5, 9, and 18 dissipative modes of the 52 available. For this case, the higher-frequency modes are also better represented by low-order models and when using a reduced-order model with 18 dissipative modes the frequency response function matches almost exactly the full-dissipative model.

Although, for a less damped structure, less dissipative modes were necessary to represent correctly its viscoelastic damping, it is worthwhile noticing that, for the structure with smaller coverage, there are less dissipative coordinates to be reduced. This is due to the fact that there are more rigid body dissipative modes, corresponding to the mechanical dof of the beam uncovered areas. Notice, however, that in both cases it is possible to reduce the number of dissipative modes to approximately one third of all non-rigid body ones. Since five ADF series terms were necessary to correctly represent the frequency dependence of the viscoelastic material, that reduction represents a gain of 300 dof (reduction from 655 to 355 dof) in the state space system for the 90% coverage case. Since the calculation of the eigenvalues of the state space matrix requires a number of operations approximately equal to N^3, where N is the matrix size, this reduction would lead to a reduction in 84% of computational effort.

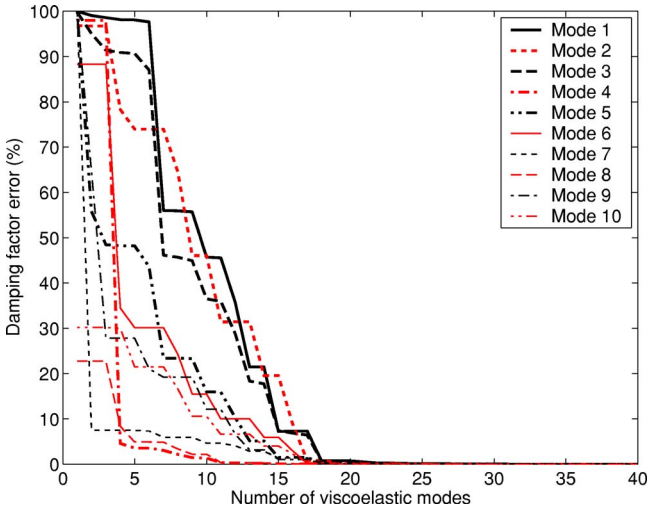

Fig. 8 Damping factor error when using different numbers of dissipative modes in second-order system compared to using all but rigid body modes

6 Conclusions

The present work has presented an alternative reduction method for internal variables-based viscoelastic finite element models. A previously developed sandwich/multilayer beam finite element model combined with the internal variables-based anelastic displacement fields viscoelastic model was used. Through a physical interpretation of the dissipative modes, due to the added internal variables, and their coupling with structural vibration modes in the second-order model, a technique for the reduction of the extra dissipative coordinates before transformation to the state space system was proposed. This method has led to much faster computations on the reduction of the state space system. Comparison between the reduced-order and full-dissipative models for a clamped beam with passive constrained layer damping treatment has shown satisfactory results. In particular, a reduction of 67% of dissipative dof has led to errors smaller than 0.5% for damping factors of the coupled structure. Similar results were obtained for the two examples considered with different treatment lengths and, thus, different levels of modal damping factors. A similar reduction can be expected for more complicated structures, although it is worthwhile to notice that the full state space system dimension depends on the number of both mechanical and dissipative dof. Hence, for structures with a large number of mechanical dof, the

second-order structural model should also be reduced prior to transformation to a state space model. The effect of also reducing the structural model, using the undamped vibration modes, on the correct representation of viscoelastic damping will be studied in a future work.

References

[1] Garg, D. P., and Anderson, G. L., 2003, "Structural Damping and Vibration Control Via Smart Sensors and Actuators," J. Vib. Control, **9**, pp. 1421–1452.

[2] Trindade, M. A., and Benjeddou, A., 2002, "Hybrid Active-Passive Damping Treatments Using Viscoelastic and Piezoelectric Materials: Review and Assessment," J. Vib. Control, **8**(6), pp. 699–746.

[3] Lesieutre, G. A., and Bianchini, E., 1995, "Time Domain Modeling of Linear Viscoelasticity Using Anelastic Displacement Fields," ASME J. Vibr. Acoust., **117**(4), pp. 424–430.

[4] Golla, D. F., and Hughes, P. C., 1985, "Dynamics of Viscoelastic Structures—A Time-Domain, Finite Element Formulation," ASME J. Appl. Mech., **52**(4), pp. 897–906.

[5] McTavish, D. J., and Hughes, P. C., 1993, "Modeling of Linear Viscoelastic Space Structures," ASME J. Vibr. Acoust., **115**, pp. 103–110.

[6] Trindade, M. A., Benjeddou, A., and Ohayon, R., 2000, "Modeling of Frequency-Dependent Viscoelastic Materials for Active-Passive Vibration Damping," ASME J. Vibr. Acoust., **122**(2), pp. 169–174.

[7] Friswell, M. I., and Inman, D. J., 1999, "Reduced-Order Models of Structures With Viscoelastic Components," AIAA J., **37**(10), pp. 1318–1325.

[8] Park, C. H., Inman, D. J., and Lam, M. J., 1999, "Model Reduction of Viscoelastic Finite Element Models," J. Sound Vib., **219**(4), pp. 619–637.

[9] Trindade, M. A., Benjeddou, A., and Ohayon, R., 2001, "Piezoelectric Active Vibration Control of Sandwich Damped Beams," J. Sound Vib., **246**(4), pp. 653–677.

[10] Friot, E., and Bouc, R., 1996, "Contrôle Optimal par Rétroaction du Rayonnement d'une Plaque Munie de Capteurs et d'Actionneurs Piézo-Électriques Non Colocalisés," 2*eme Colloque GDR Vibroacoustique*, LMA, Marseille pp. 229–248.

[11] Trindade, M. A., Benjeddou, A., and Ohayon, R., 2001, "Finite Element Modeling of Hybrid Active-Passive Vibration Damping of Multilayer Piezoelectric Sandwich Beams. Part 1: Formulation and Part 2: System Analysis," Int. J. Numer. Methods Eng., **51**(7), pp. 835–864.